Supporting Information

Reaction of a Cp*Ir(III) Cation with mono- and di-lacunary Keggin-type heteropolytungstates, and dimer of hexa-lacunary Dawson-type phosphopolytungstate

Sugiarto, Jun Shinogi, Sherif E. Ebied, Dachao Hong, Yoshihiro Kon, and Masahiro Sadakane*

Table S1. Crystallographic parameters. *Note that formulas and formula weights are based on X-ray diffraction results.

	$SiW_{10}O_{36}Cp^*Ir$	**$SiW_{11}O_{39}(Cp^*Ir)_2Cl$**	**$PW_{11}O_{39}(Cp^*Ir)_2Cl$**	**$P_8W_{48}O_{184}(Cp^*Ir)_4$-dimer**
Formula unit*	$C_{40}H_{60}Ir_4K_{23}O_{156}Si_4W_{40}$	$C_{20}ClIr_2K_5O_{52.6}SiW_{11}$	$C_{20}ClIr_2K_{3.4}O_{47.63}PW_{11}$	$C_{40}Ir_4K_{29.8}O_{257.31}P_8W_{48.62}$
Formula weight* (g/mol)	12171.34	3747.59	3608.34	15717.22
Crystal system	Tetragonal	Monoclinic	Tetragonal	Triclinic
Space group (number)	$I\bar{4}$ (82)	$C2_1/m$ (12)	$I4/m$ (87)	$P\bar{1}$ (2)
a, Å	31.071(3)	22.395(2)	35.1781(13)	17.555(2)
b, Å	31.071(3)	11.533(1)	35.1781(13)	22.843(2)
c, Å	18.191(2)	27.827(2)	11.3965(6)	23.043(2)
α, °	90	90	90	65.373(1)
β, °	90	104.913(1)	90	67.697(1)
γ, °	90	90	90	85.608(1)
V, Å^3	14665(3)	6945.2(9)	14103.2(13)	7734.8(12)
Z	2	4	8	1
D_{calc} (g/cm^3)	2.756	3.584	3.399	3.374
μ (mm^{-1})	17.830	22.403	21.966	20.249
Radiation	Mo Kα (λ = 0.71073 Å)	Mo Kα (λ = 0.71073 Å)	Mo Kα (λ = 0.71073 Å)	Mo Kα (λ = 0.71073 Å)
Temperature (K)	100(2)	123(2)	123(2)	123(2)
F_{000}	10618	6539	12525	6890
Θ range	1.492 to 25.420°	1.515 to 27.943°	1.637 to 27.539°	1.260 to 27.487°
Index ranges	−33 ≤ h ≤ 37 −30 ≤ k ≤ 37 −18 ≤ l ≤ 16	−29 ≤ h ≤ 29 −15 ≤ k ≤ 15 −36 ≤ l ≤ 36	−37 ≤ h ≤ 45 −34 ≤ k ≤ 45 −14 ≤ l ≤ 13	−22 ≤ h ≤ 22 −29 ≤ k ≤ 29 −29 ≤ l ≤ 29
No. of reflections collected	35539	41261	35955	90891
Unique reflections (R_{int})	13480 (0.0511)	8666 (0.0372)	8541 (0.0548)	35055 (0.0338)
Data/restrains/parameters	13480/515/652	8666/608/501	8541/741/484	35055/445/1897
R indexes [I>2σ(I)]	$R_1{}^a$ = 0.0498 $wR_2{}^b$ = 0.1226	R_1 = 0.0675 wR_2 = 0.1405	R_1 = 0.0519 wR_2 = 0.1055	R_1 = 0.0331 wR_2 = 0.0788
R indexes (all data)	R_1 = 0.0718 wR_2 = 0.1343	R_1 = 0.0722 wR_2 = 0.1422	R_1 = 0.0692 wR_2 = 0.1119	R_1 = 0.0453 wR_2 = 0.0836
Goodness-of-fit	1.013	1.257	1.077	1.030
$(\Delta/\sigma)_{max}$	0.000	0.000	0.003	0.003
$\Delta\rho_{max/min}$ (e A^{-3})	3.743/−3.187	4.018/−4.354	2.426/−3.144	2.351/−3.162
CCDC number	2356622	2356623	2356624	2356625

$^aR_1 = \{\Sigma||F_o|-|F_c||\}/\{\Sigma|F_o|\}$; $^bwR_2 = [\Sigma w(F_o^2-F_c^2)/\Sigma wF_o^2]^{1/2}$

Table S2. BVS calculation results showing the oxidation state of W, Si, and P atoms and the protonation state of O atoms in **IrSiW10**, **Ir2SiW11**, and **Ir2PW11**.

$SiW_{10}O_{36}Cp^*Ir$				**$SiW_{11}O_{39}(Cp^*Ir)_2Cl$**				**$PW_{11}O_{39}(Cp^*Ir)_2Cl$**			
W1	5.74	W6	5.81	W1	6.01	W5	6.27	W1	6.01	W5	6.09
W2	5.70	W7	5.78	W2	6.23	W6	6.35	W2	5.93	W6	6.13
W3	5.90	W8	6.28	W3	5.95	W7	6.12	W3	6.24	W7	6.14
W4	6.01	W9	6.14	W4	5.75			W4	6.14		
W5	5.94	W10	5.98								
				Si1	4.00	O12	1.98	P1	4.92	O8	1.84
Si1	3.89	O19	1.80	O1	1.94	O13	2.07	O1P	1.92	O9	2.00
O1	1.57	O20	1.77	O2	1.93	O14	1.97	O2P	1.97	O10	2.96
O2	1.92	O21	1.77	O3	1.76	O15	1.84	O3P	1.75	O11	1.84
O3	1.74	O22	2.05	O4	1.75	O16	1.78	O4P	1.78	O12	2.05
O4	1.94	O23	1.62	O5	2.16	O17	1.99	O1	1.94	O13	2.08
O5	1.81	O24	1.95	O6	2.31	O18	2.07	O2	2.00	O14	2.02
O6	1.57	O25	1.66	O7	2.06	O19	1.93	O3	1.76	O15	1.77
O7	1.99	O26	1.66	O8	1.79	O20	1.84	O4	1.81	O16	1.81
O8	1.49	O27	1.81	O9	2.12	O21	1.69	O5	2.09	O17	2.09
O9	1.72	O28	1.93	O10	2.01	O22	1.68	O6	2.12	O18	2.04
O10	1.77	O29	1.75	O11	1.74	O23	1.88	O7	2.09	O19	1.81
O11	2.10	O30	1.82								
O12	1.95	O31	1.94								
O13	1.78	O32	1.91								
O14	1.88	O33	1.61								
O15	1.95	O34	1.53								
O16	1.57	O35	1.51								
O17	1.70	O36	1.85								
O18	1.91										

Table S3. BVS calculation results showing the oxidation state of W, Si, and P atoms and the protonation state of O atoms **$P_8W_{48}O_{184}(Cp^*Ir)_4$-dimer**The BVS values of W25 and W26 were not calculated because some of the required oxo/aquo ligands could not be located.

$P_8W_{48}O_{184}(Cp^*Ir)_4$-dimer									
W1	5.93	W6	5.97	W11	5.87	W16	5.91	W21	5.96
W2	5.96	W7	5.92	W12	5.90	W17	5.93	W22	5.98
W3	5.97	W8	5.96	W13	5.90	W18	5.90	W23	5.97
W4	5.96	W9	5.89	W14	5.84	W19	5.89	W24	5.88
W5	5.96	W10	5.98	W15	5.95	W20	6.01		
P1	4.91	O17	1.68	O37	2.47	O57	2.42	O77	1.60
P2	4.93	O18	1.63	O38	2.22	O58	2.38	O78	1.69
P3	4.91	O19	1.82	O39	1.95	O59	1.59	O79	1.90
P4	4.91	O20	1.95	O40	1.87	O60	1.78	O80	1.92
O1	1.88	O21	1.65	O41	1.92	O61	1.78	O81	1.96
O2	1.91	O22	1.92	O42	1.80	O62	1.58	O82	1.62
O3	1.89	O23	2.04	O43	1.83	O63	1.91	O83	1.85
O4	1.87	O24	2.08	O44	1.70	O64	1.93	O84	1.60
O5	1.93	O25	1.90	O45	1.79	O65	1.91	O85	1.84
O6	1.66	O26	1.96	O46	1.62	O66	1.61	O86	1.81
O7	1.93	O27	1.60	O47	1.89	O67	1.79	O87	1.89
O8	1.63	O28	1.85	O48	1.61	O68	1.57	O88	1.90
O9	1.86	O29	1.58	O49	1.64	O69	1.99	O89	1.91
O10	1.83	O30	1.94	O50	1.84	O70	1.91	O90	1.63
O11	1.63	O31	1.93	O51	1.65	O71	2.09	O91	1.81
O12	1.73	O32	1.87	O52	1.92	O72	2.06	O92	1.64
O13	1.74	O33	1.64	O53	1.85	O73	1.67	O93	0.95
O14	1.92	O34	1.77	O54	1.90	O74	1.76	OA	1.49
O15	1.80	O35	1.80	O55	1.83	O75	1.75	OB	0.39
O16	1.69	O36	1.55	O56	1.80	O76	1.72	OC	1.43

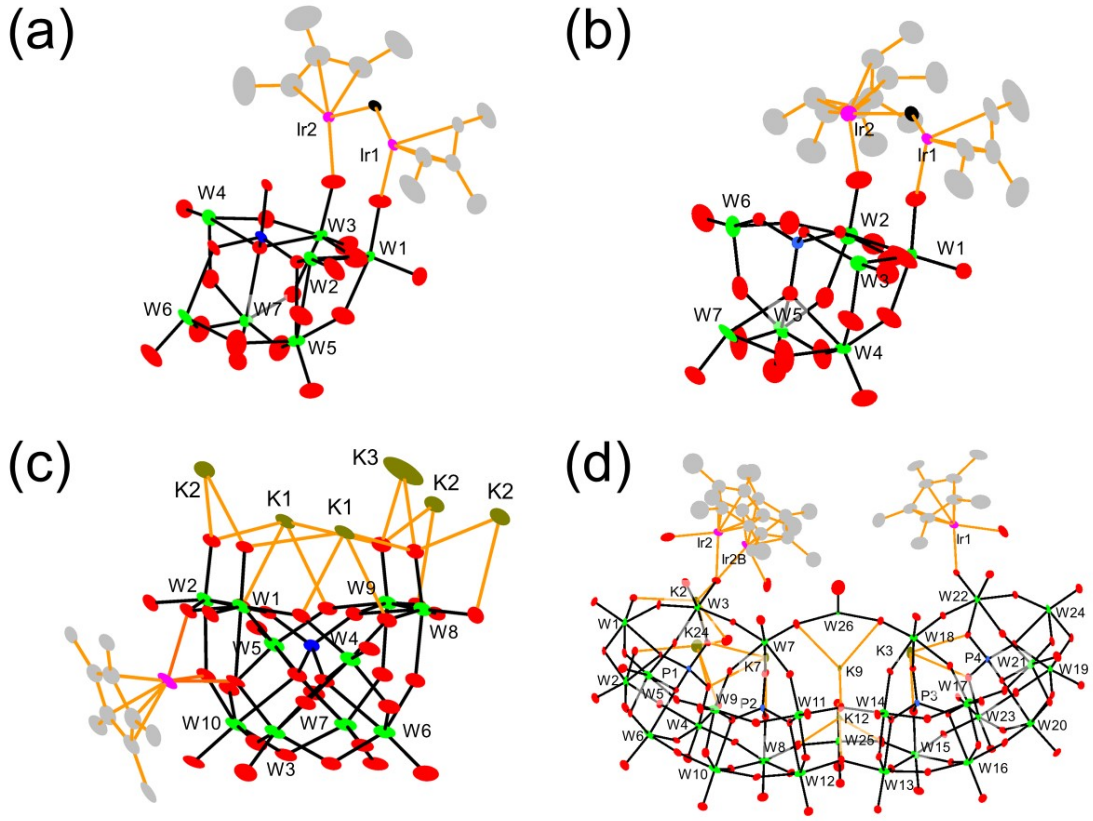

Figure S1. Thermal ellipsoidal (50% probability) representation of polyoxotungstate with Cp*Ir and some K cations in the asymmetric units of (a) $K_5[\alpha\text{-}SiW_{11}O_{39}(Cp^*Ir)_2Cl]$, (b) $K_{3.75}(Cp^*Ir)_2(OH)_3)_{0.25}[\alpha\text{-}PW_{11}O_{39}(Cp^*Ir)_2Cl]$, (c) $K_6[\gamma\text{-}SiW_{10}O_{36}(Cp^*Ir)]$ and (d) $K_{30.8}[P_8W_{48}O_{184}(Cp^*Ir(H_2O))_4(WO_2(H_2O)_2)_{0.6}]$. Green, blue, pink, grey, red, black balls and dark green balls represent W, Si (or P), Ir, C, O, Cl and K, respectively.

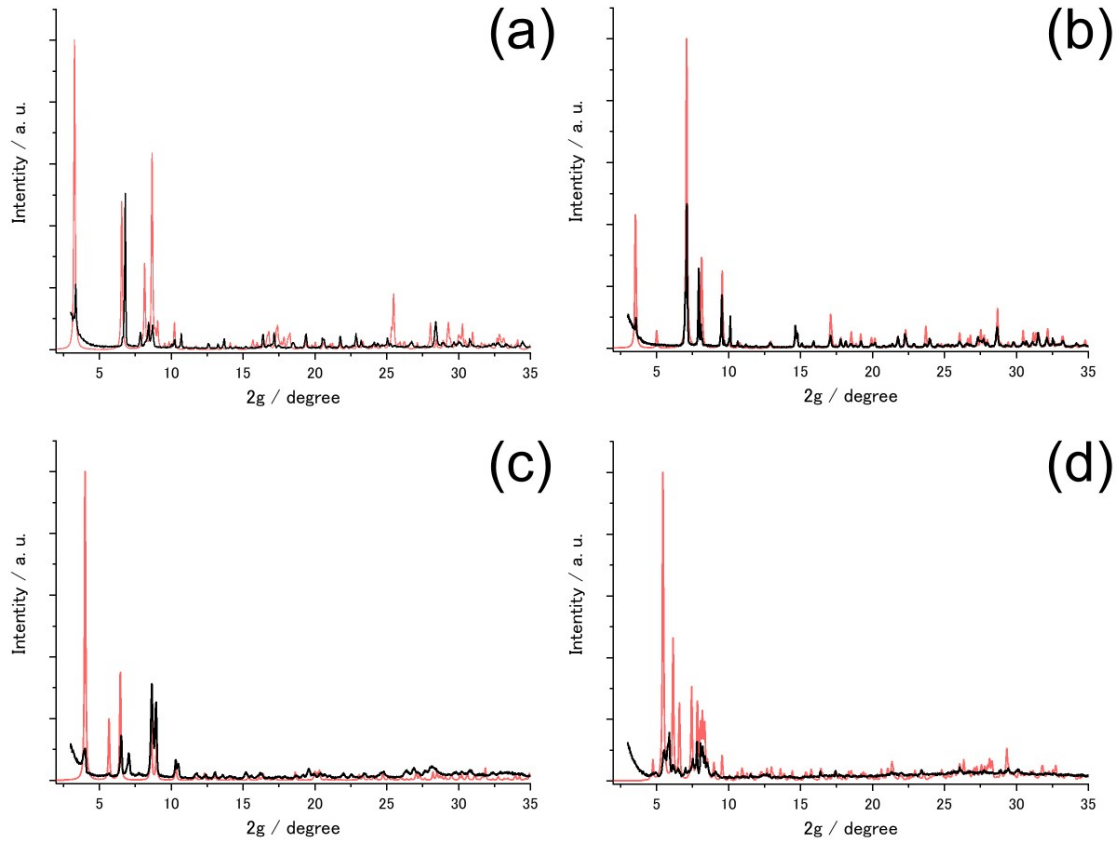

Figure S2. A room temperature powder X-ray diffraction pattern of (a) $K_5[\alpha\text{-}SiW_{11}O_{39}(Cp^*Ir)_2Cl]$, (b) $K_{3.75}(Cp^*Ir)_2(OH)_3)_{0.25}[\alpha\text{-}PW_{11}O_{39}(Cp^*Ir)_2Cl]$, (c) $K_6[\gamma\text{-}SiW_{10}O_{36}(Cp^*Ir)]$ and (d) $K_{30.8}[P_8W_{48}O_{184}(Cp^*Ir(H_2O))_4(WO_2(H_2O)_2)_{0.6}]$. Black and red lines represent observed and simulated pattern using single crystal structure, respectively.

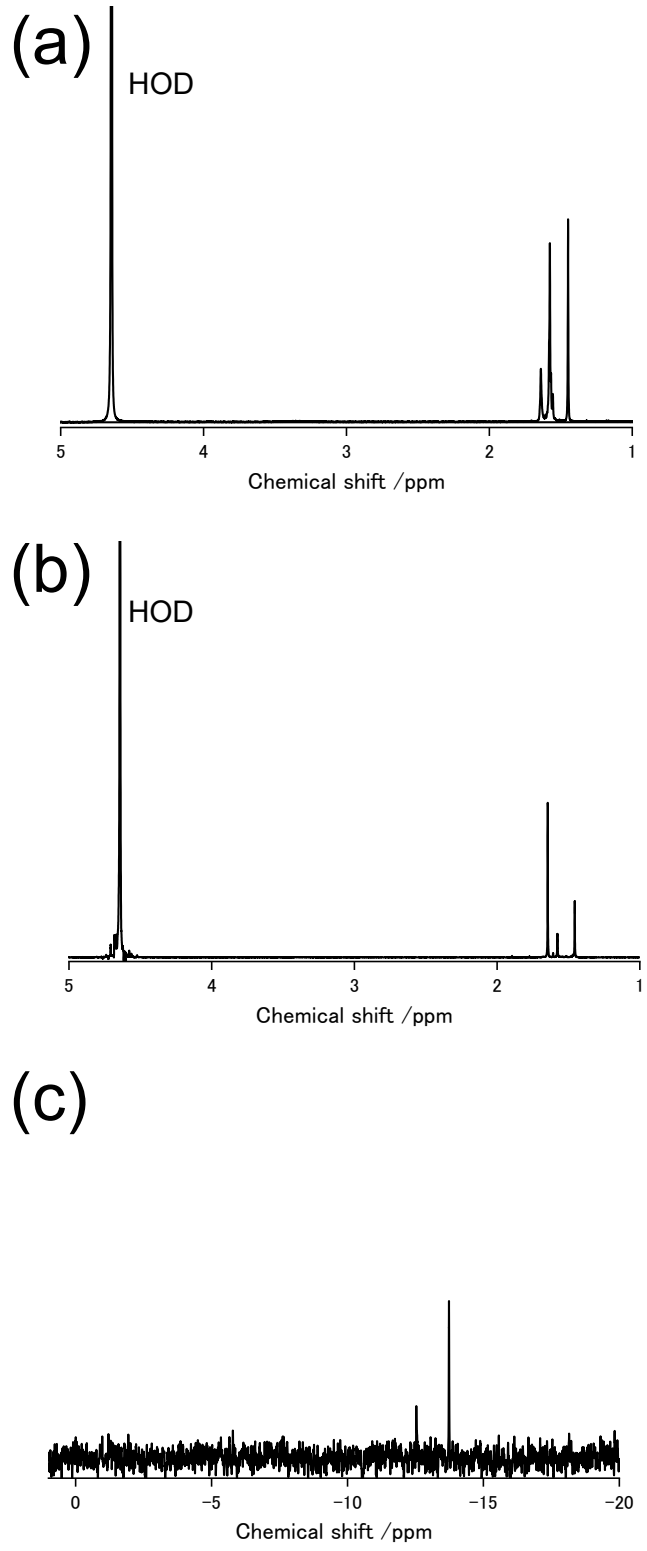

Figure S3. ^{1}H NMR spectrum of (a) $K_5[SiW_{11}O_{39}(Cp^*Ir)_2Cl]$, (b) $K_4[PW_{11}O_{39}(Cp^*Ir)_2Cl]$ in D_2O, and (c) ^{31}P NMR spectrum of $K_4[PW_{11}O_{39}(Cp^*Ir)_2Cl]$ in D_2O.

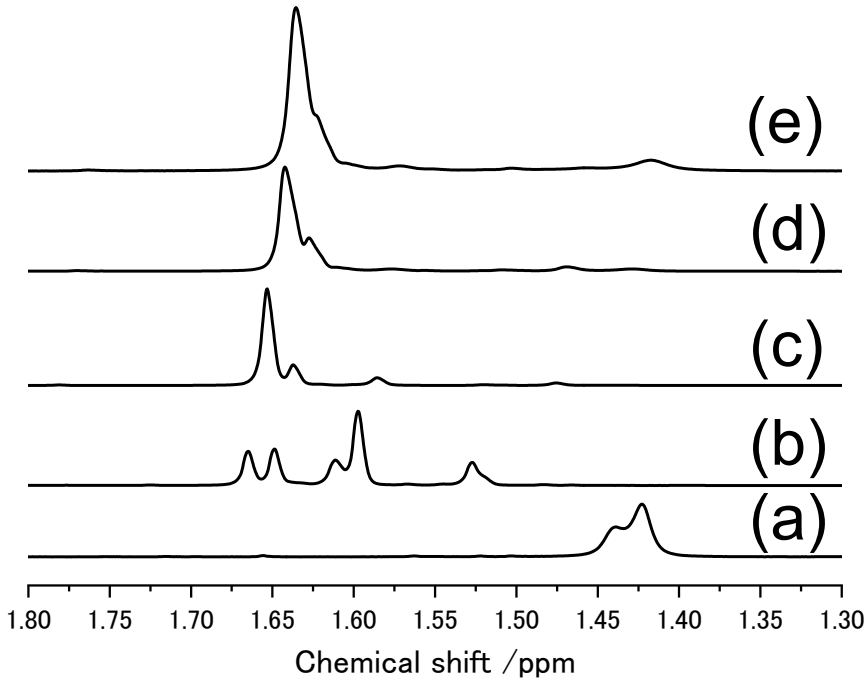

Figure S4. ^{1}H NMR spectrum of a D_2O solution containing (a) $[Cp^*IrCl_2]_2$, and $K_8[\alpha\text{-}SiW_{11}O_{39}]$ and $[Cp^*IrCl_2]_2$ with different $Cp^*Ir/[\gamma\text{-}SiW_{11}O_{39}]^{8-}$ ratios of (b) 0.5, (c) 1.0, (d) 2, and (e) 4.

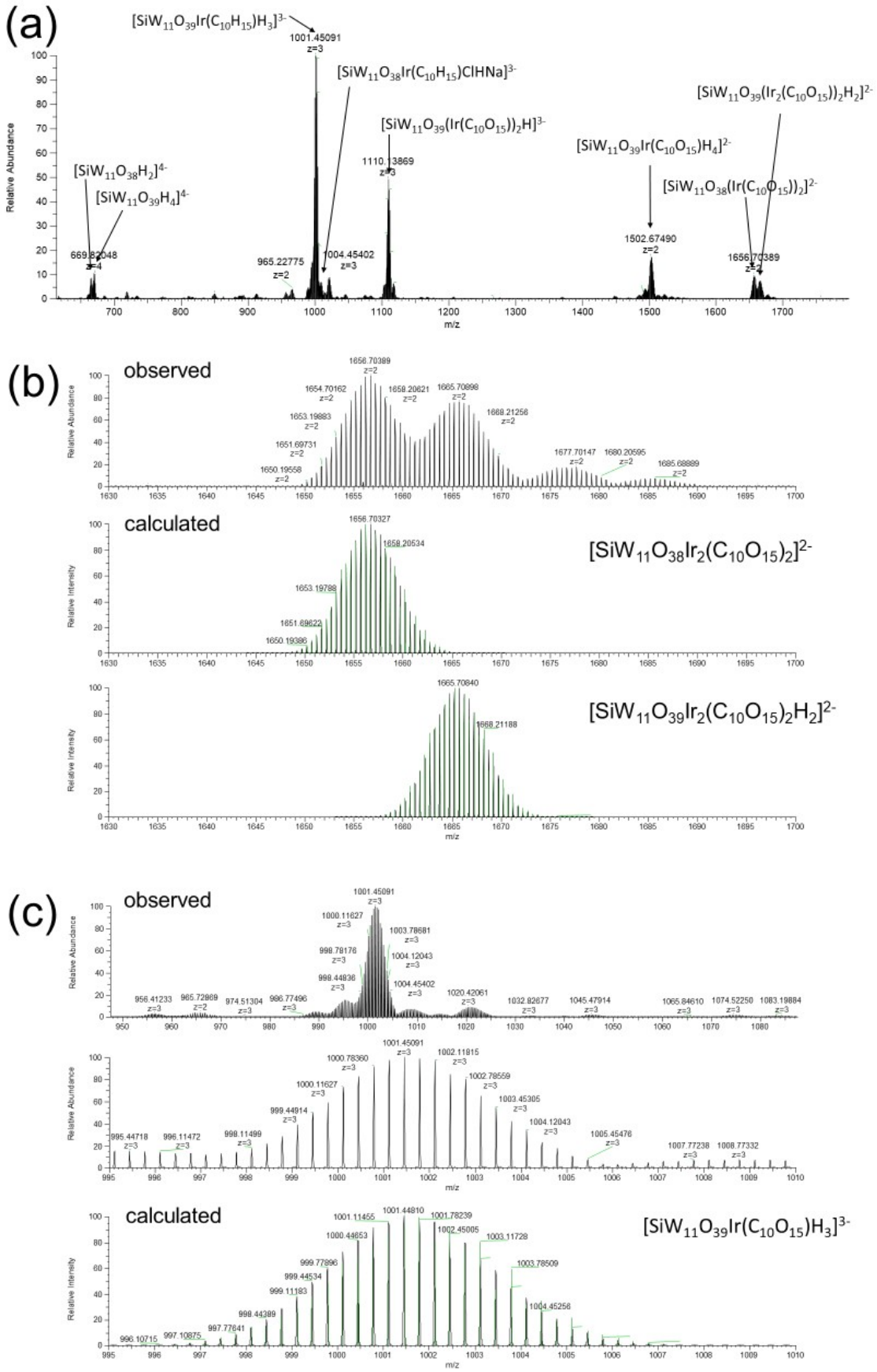
(a)
[SiW11O39Ir(C10H15)H3]3-
1001.45091
z=3
[SiW11O38Ir(C10H15)ClHNa]3-
[SiW11O39(Ir(C10O15))2H]3-
[SiW11O39Ir(C10O15)H4]2-
[SiW11O39(Ir2(C10O15))2H2]2-
[SiW11O38H2]4-
[SiW11O39H4]4-
1110.13869
z=3
[SiW11O38(Ir(C10O15))2]2-
1502.67490
z=2
1656.70389
z=2
669.82048
z=4
965.22775
z=2
1004.45402
z=3
Relative Abundance
m/z
(b)
observed
1656.70389
z=2
1654.70162
z=2
1658.20621
z=2
1665.70898
z=2
1653.19883
z=2
1668.21256
z=2
1651.69731
z=2
1677.70147
z=2
1680.20595
z=2
1650.19558
z=2
1685.68889
z=2
calculated
1656.70327
1658.20534
[SiW11O38Ir2(C10O15)2]2-
1653.19788
1651.69622
1650.19386
1665.70840
1668.21188
[SiW11O39Ir2(C10O15)2H2]2-
Relative Intensity
m/z
(c)
observed
1001.45091
z=3
1000.11627
z=3
1003.78681
z=3
998.78178
z=3
1004.12043
z=3
998.44836
z=3
1004.45402
z=3
1020.42061
z=3
956.41233
z=3
985.72889
z=2
974.51304
z=3
986.77496
z=3
1032.82677
z=3
1045.47914
z=3
1065.84610
z=3
1074.52250
z=3
1083.19884
z=3
1001.45091
z=3
1002.11815
z=3
1000.78360
z=3
1002.78559
z=3
1000.11627
z=3
1003.45305
z=3
999.44914
z=3
1004.12043
z=3
995.44718
z=3
996.11472
z=3
999.11499
z=3
1005.45476
z=3
1007.77238
z=3
1008.77332
z=3
calculated
1001.44810
1001.11455
1001.78239
1000.44853
1002.45005
1003.11728
999.77896
1003.78509
999.44534
999.11183
1004.45256
998.44389
997.77841
997.10875
996.10715
[SiW11O39Ir(C10O15)H3]3-
Relative Abundance
Relative Intensity
m/z

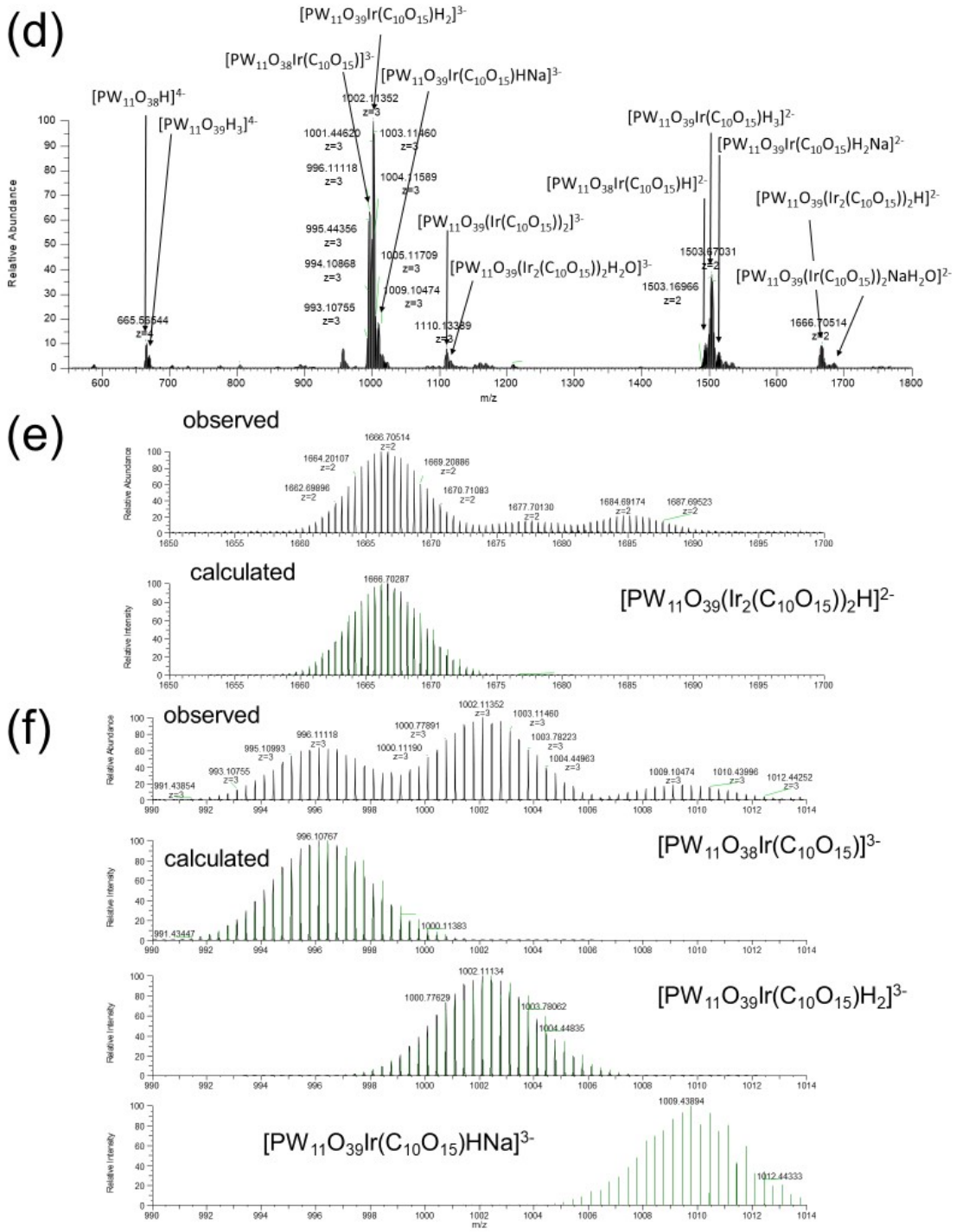

Figure S5. High-resolution ESI-MS of (a) - (c) $K_5[\alpha\text{-}SiW_{11}O_{39}(Cp^*Ir)_2Cl]$. ((a) m/z between 600 and 1800 together with peak assignments, (b) and (c) enlarged profiles together with calculated profiles) and (d) - (f) $K_{3.75}(Cp^*Ir)_2(OH)_3)_{0.25}[\alpha\text{-}PW_{11}O_{39}(Cp^*Ir)_2Cl]$ ((d) m/z between 550 and 1800 together with peak assignments, (e) and (f) enlarged profiles together with calculated profiles).

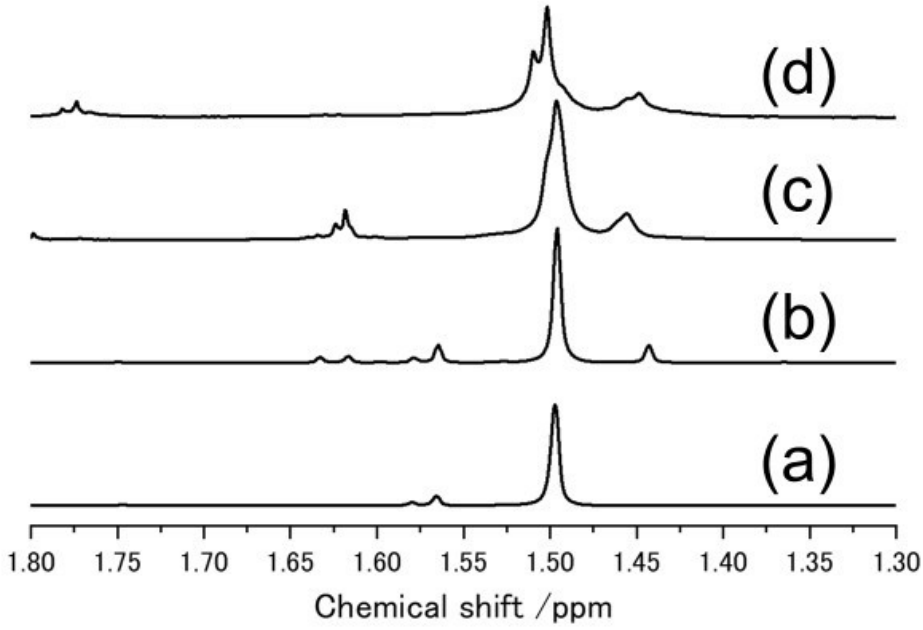

Figure S6. ^{1}H NMR spectrum of a D_2O solution containing $K_8[\gamma\text{-}SiW_{10}O_{36}]\text{-}12H_2O$ and $[Cp^*IrCl_2]_2$ with different $Cp^*Ir/[\gamma\text{-}SiW_{10}O_{36}]^{6-}$ ratios of (a) 0.5, (b) 1.0, (c) 2, and (d) 4.

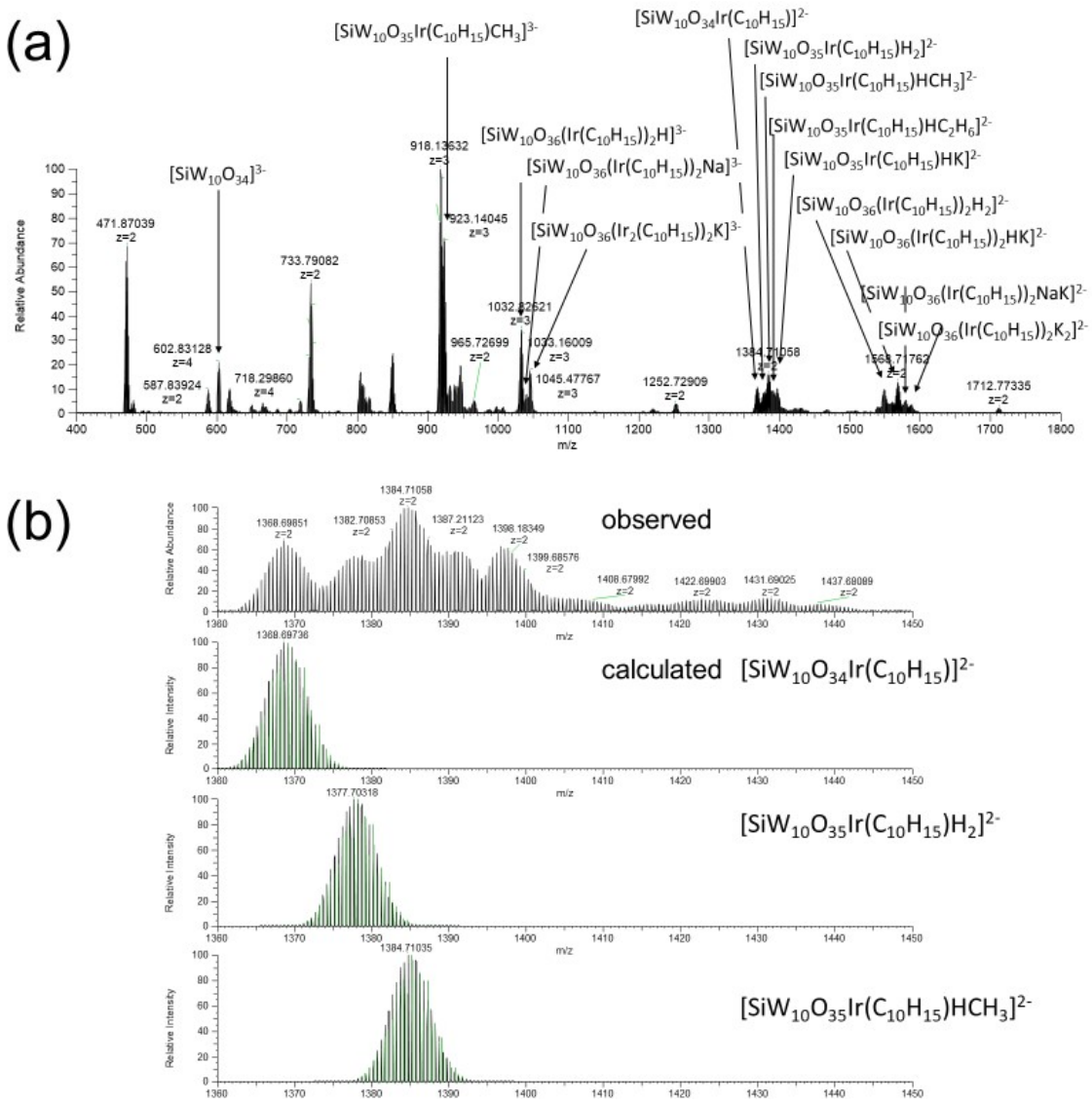
(a)
[SiW10O35Ir(C10H15)CH3]3-
[SiW10O34Ir(C10H15)]2-
[SiW10O35Ir(C10H15)H2]2-
[SiW10O35Ir(C10H15)HCH3]2-
[SiW10O35Ir(C10H15)HC2H6]2-
[SiW10O35Ir(C10H15)HK]2-
[SiW10O36(Ir(C10H15))2H2]2-
[SiW10O36(Ir(C10H15))2HK]2-
[SiW10O36(Ir(C10H15))2NaK]2-
[SiW10O36(Ir(C10H15))2K2]2-
[SiW10O36(Ir(C10H15))2H]3-
[SiW10O36(Ir(C10H15))2Na]3-
[SiW10O36(Ir2(C10H15))2K]3-
[SiW10O34]3-
918.13632 z=3
923.14045 z=3
471.87039 z=2
733.79082 z=2
602.83128 z=4
587.83924 z=2
718.29860 z=4
965.72699 z=2
1032.82621 z=3
1033.16009 z=3
1045.47767 z=3
1252.72909 z=2
1384.71058 z=2
1712.77335 z=2
Relative Abundance
m/z
(b)
observed
1384.71058 z=2
1368.69851 z=2
1382.70853 z=2
1387.21123 z=2
1398.18349 z=2
1399.68576 z=2
1408.67992 z=2
1422.69903 z=2
1431.69025 z=2
1437.68089 z=2
calculated [SiW10O34Ir(C10H15)]2-
1368.69736
[SiW10O35Ir(C10H15)H2]2-
1377.70318
[SiW10O35Ir(C10H15)HCH3]2-
1384.71035
Relative Intensity
m/z

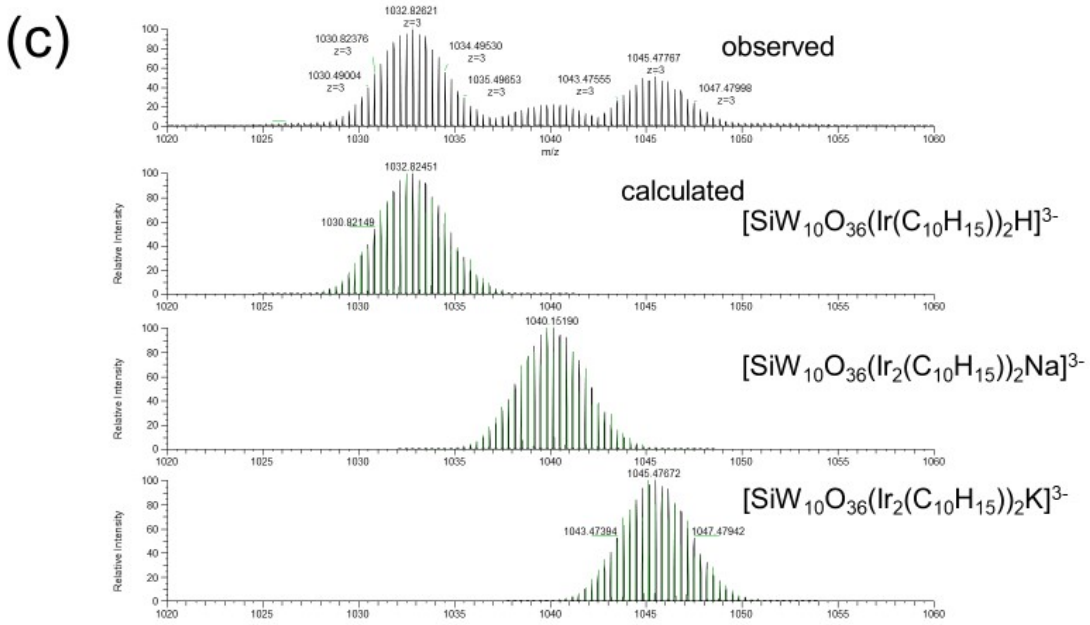

Figure S7. High-resolution ESI-MS of $K_6[\gamma\text{-}SiW_{10}O_{36}(Cp^*Ir)]$. (a) m/z between 400 and 1800 together with peak assignments, (b) and (c) enlarged profiles together with calculated profiles.

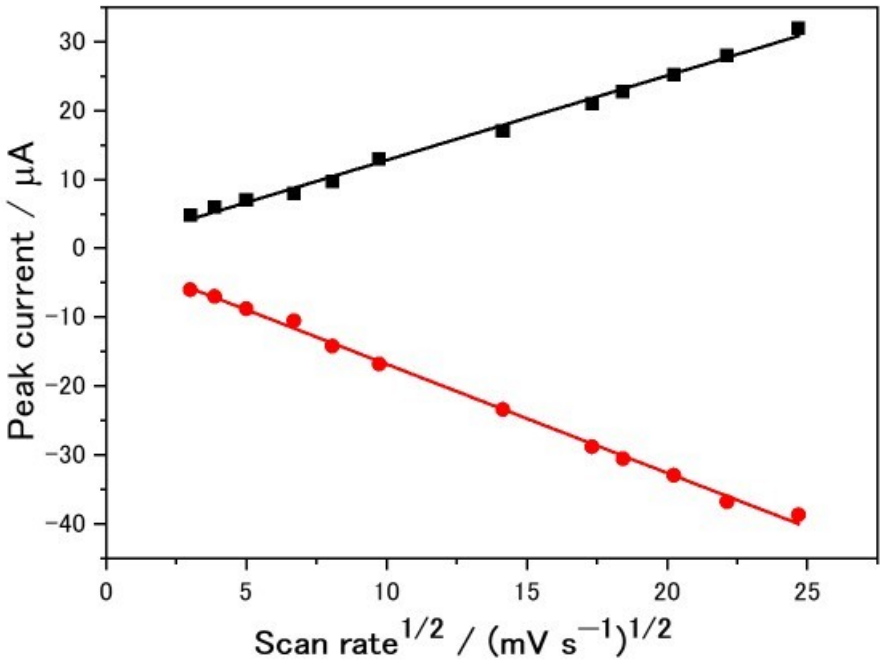

Figure S8. Relationship between peak currents and scan rate of the reversible redox couple at -688 mV. (black) anodic current and (red) cathodic current.

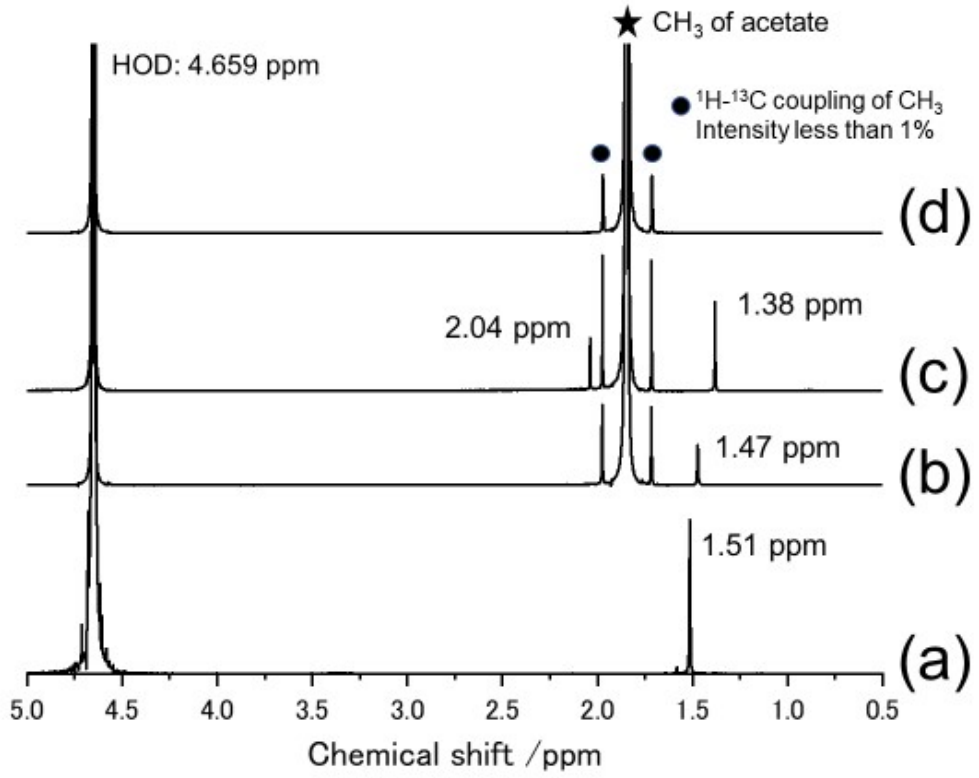

Figure S9. ^{1}H NMR of (a) $K_6[\gamma\text{-}SiW_{10}O_{36}(Cp^*Ir)]$ in D_2O, (b) $K_6[\gamma\text{-}SiW_{10}O_{36}(Cp^*Ir)]$ (1 mM) in the acetate buffer (pD 4.7), (c) $[Cp^*IrCl_2]_2$ (1 mM) in the acetate buffer (pD 4.7), and (d) the acetate buffer (pD 4.7). The acetate buffer (pD 4.7) was prepared by mixing 1.0 M AcOH in D_2O and 1.0 M AcONa in D_2O to adjust pH value of a pH-meter at 4.3 (pD = pH + 0.4).

nt.

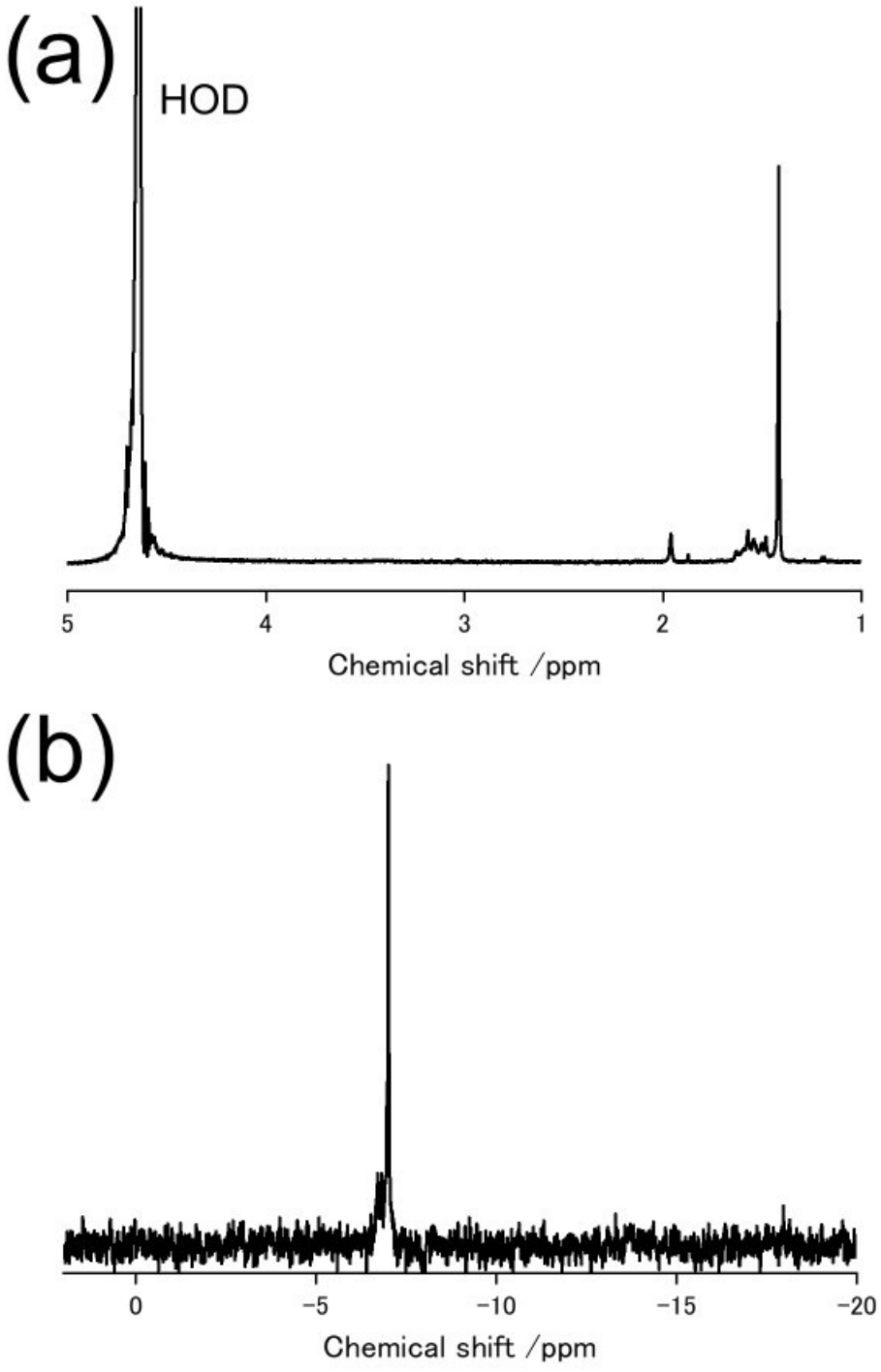

Figure S10. (a) ^{1}H NMR spectrum and (b) ^{31}P NMR spectrum of $[P_8W_{48}O_{184}(WO_2(H_2O)_2)_{0.6}(Cp^*Ir(H_2O))_4]^{30.8-}$ from dimeric $[P_4W_{24}O_{94}]^{24-}$ in 1.0 M of LiCl in D_2O. The $[P_8W_{48}O_{184}(Cp^*Ir)_4]$ compound did not dissolve in D_2O.

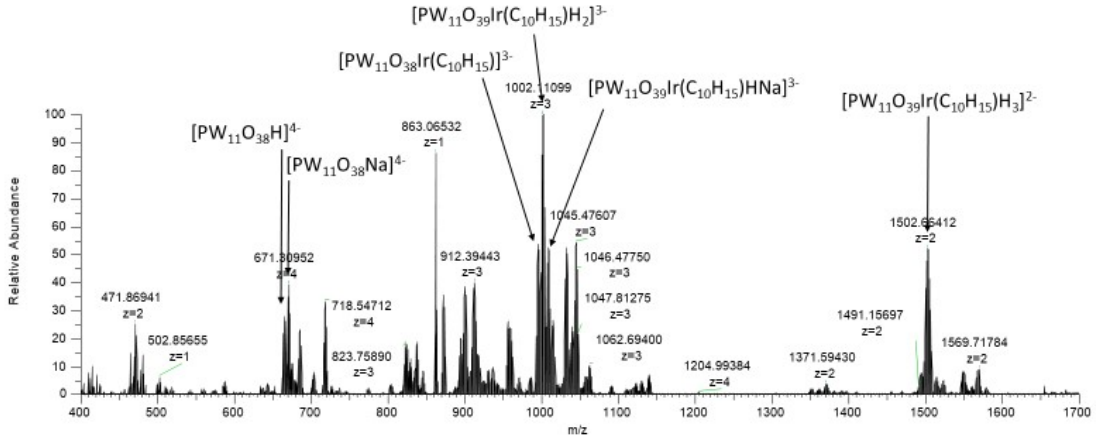

Figure S11. High-resolution ESI-MS of $K_{30.8}[P_8W_{48}O_{184}(Cp^*Ir(H_2O))_4(WO_2(H_2O)_2)_{0.6}]$ together with assignments.

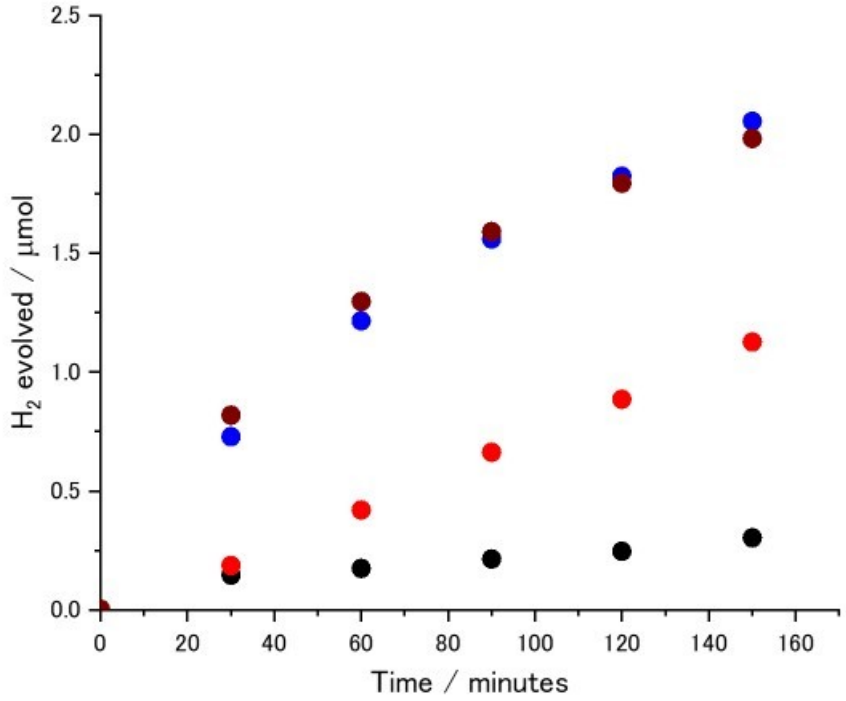

Figure S12. H_2 evolution activity using same amount of Cp*Ir. (black) $[Cp^*IrCl_2]_2$ dissolved in CH_3CN was injected, (brown) $[Cp^*IrCl_2]_2$ dissolved in H_2O was injected, (red) $K_6[\gamma\text{-}SiW_{10}O_{36}(Cp^*Ir)]$, and (blue) $K_6[\gamma\text{-}SiW_{11}O_{39}(Cp^*Ir)_2Cl]$. Reaction was proceeded in the presence of 0.2 μmol of Cp*Ir in 0.1 M formate buffer (pH 3.6, 5 mL) at 25 °C.

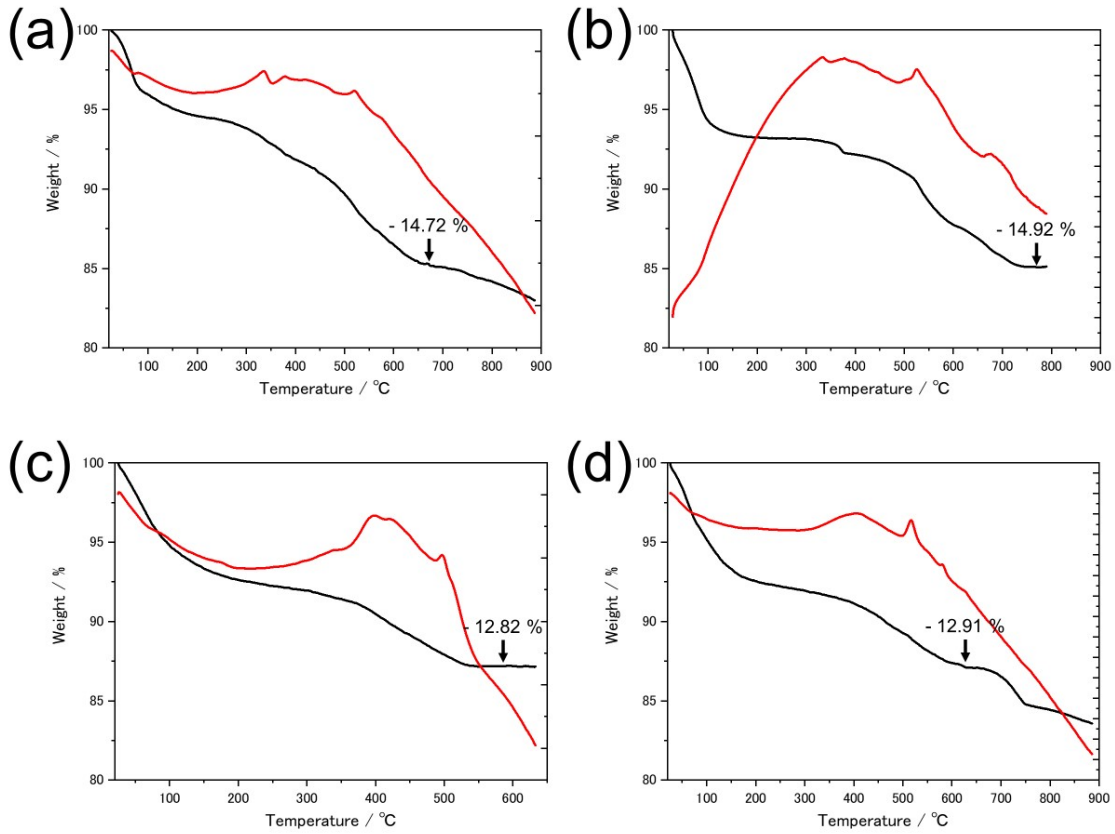

Figure S13 TG-DTA profiles of (a) $K_5[\alpha\text{-}SiW_{11}O_{39}(Cp^*Ir)_2Cl]$, (b) $K_{3.75}(Cp^*Ir)_2(OH)_3)_{0.25}[\alpha\text{-}PW_{11}O_{39}(Cp^*Ir)_2Cl]$, (c) $K_6[\gamma\text{-}SiW_{10}O_{36}(Cp^*Ir)]$ and (d) $K_{30.8}[P_8W_{48}O_{184}(Cp^*Ir(H_2O))_4(WO_2(H_2O)_2)_{0.6}]$ under air flow.

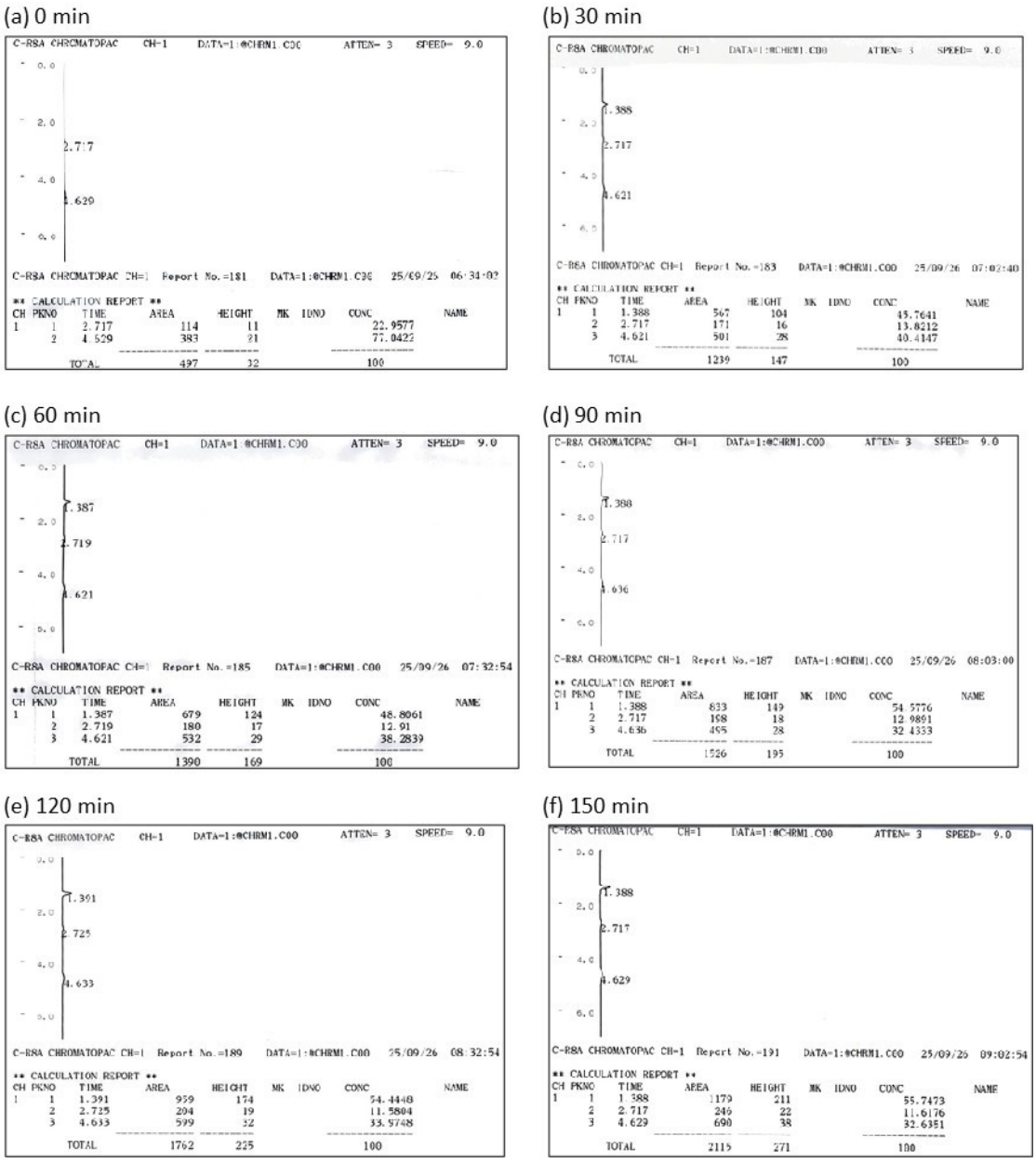

Figure S14. GC data of H_2 evolution. $[Cp^*IrCl_2]_2$ dissolved in CH_3CN (0.2 μmol of Ir, 40 mL) was injected into 0.1 M formate buffer (pH 3.6, 5 mL) at 25 °C.

(a) 0 min

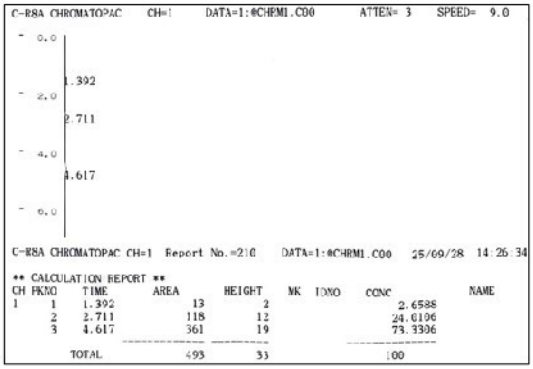

(b) 30 min

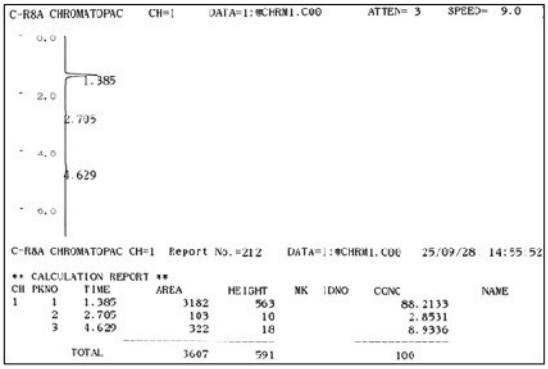

(c) 60 min

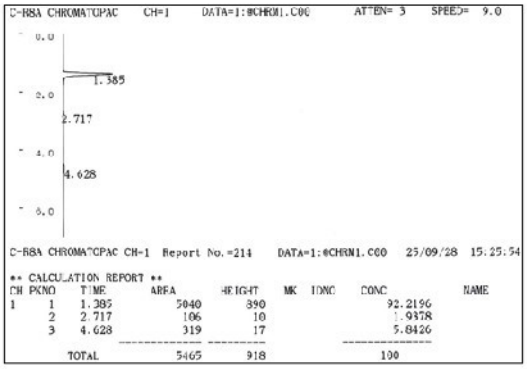

(d) 90 min

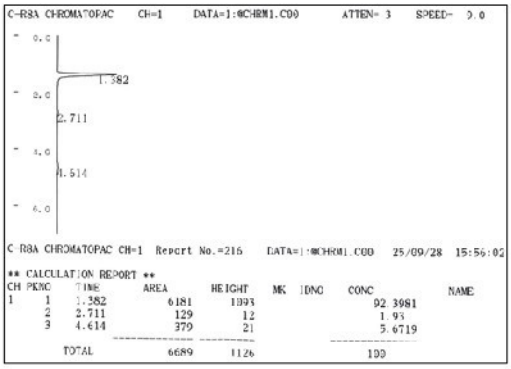

(e) 120 min

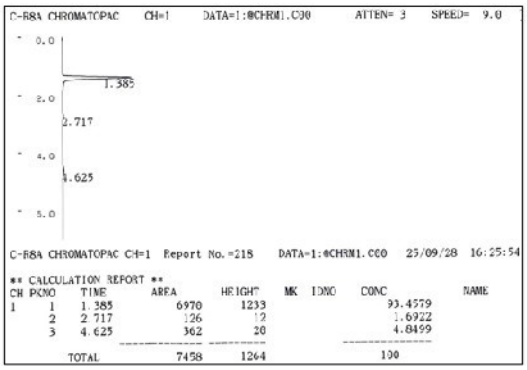

(f) 150 min

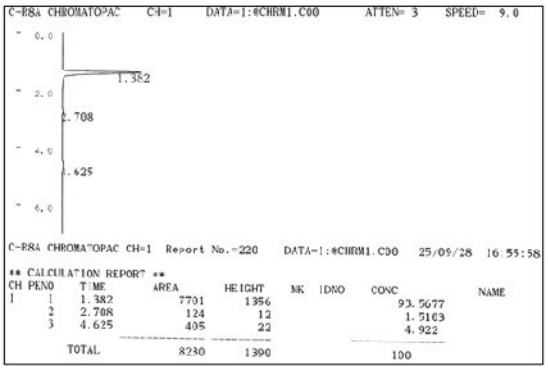

Figure S15. GC data of H_2 evolution. $[Cp^*IrCl_2]_2$ dissolved in H_2O (0.2 μmol of Ir, 40 mL) was injected into 0.1 M formate buffer (pH 3.6, 5 mL) at 25 °C.

(a) 0 min

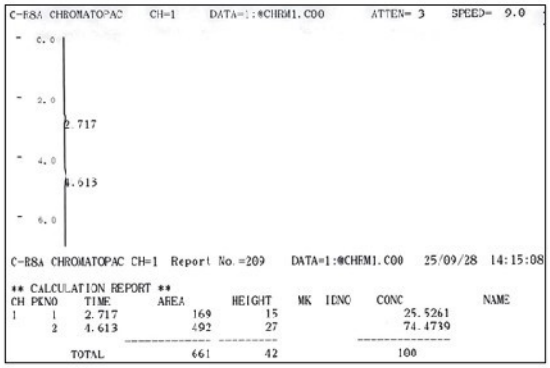

(b) 30 min

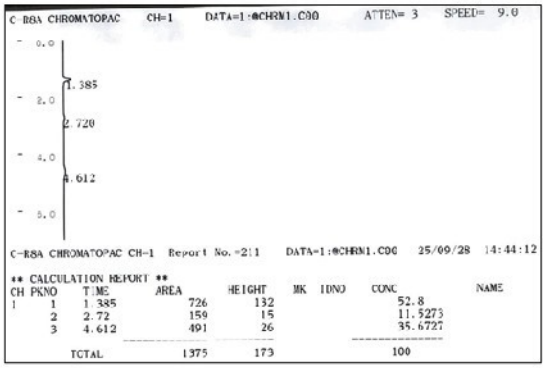

(c) 60 min

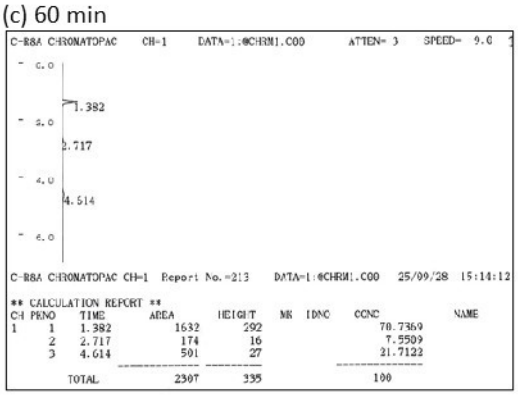

(d) 90 min

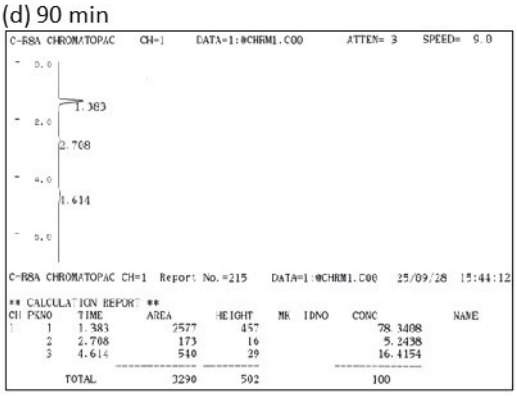

(e) 120 min

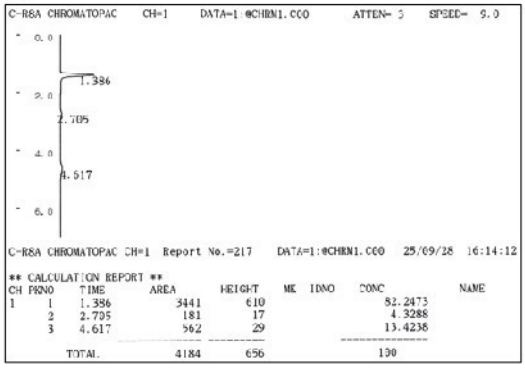

(f) 150 min

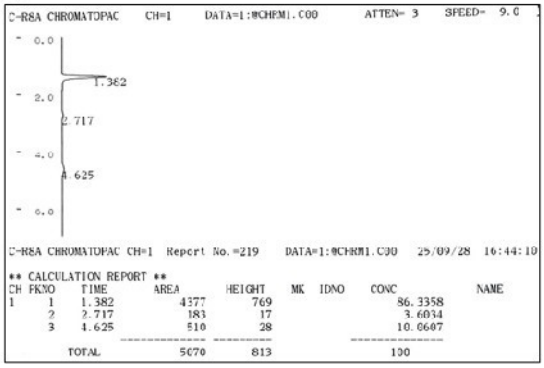

Figure S16. GC data of H_2 evolution. $K_6[\gamma\text{-}SiW_{10}O_{36}(Cp^*Ir)]$ dissolved in H_2O (0.2 μmol of Ir, 40 mL) was injected into 0.1 M formate buffer (pH 3.6, 5 mL) at 25 °C.

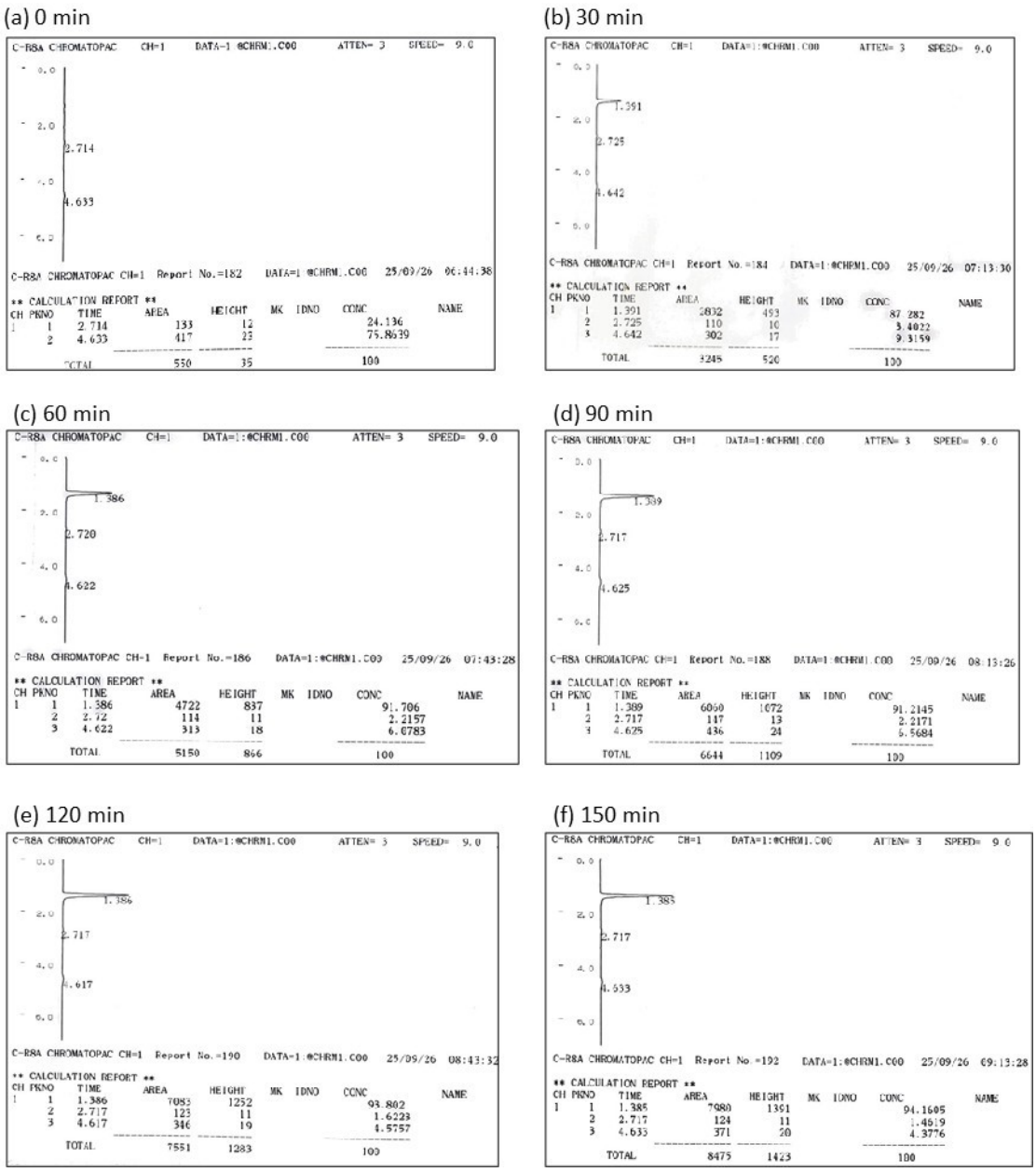

Figure S17. GC data of H_2 evolution. $K_6[\gamma\text{-}SiW_{11}O_{39}(Cp^*Ir)_2Cl]$ dissolved in H_2O (0.2 μmol of Ir, 40 mL) was injected into 0.1 M formate buffer (pH 3.6, 5 mL) at 25 °C.